

Tip-enhanced Raman scattering of *p*-thiocresol molecules on individual gold nanoparticles

Jianing Chen,^{1,2} Weisheng Yang,¹ Kimberly Dick,³ Knut Deppert,³ H. Q. Xu,³ Lars Samuelson,³ and Hongxing Xu^{1,3,a)}

¹Beijing National Laboratory for Condensed Matter Physics, Institute of Physics, Chinese Academy of Sciences, P.O. Box 603-146, Beijing 100080, People's Republic of China

²School of Physics and Optoelectronics, Dalian University of Technology, Dalian 116024, People's Republic of China

³Division of Solid State Physics, Lund University, P.O. Box 118, SE-22100, Sweden

(Received 20 November 2007; accepted 3 January 2008; published online 5 March 2008)

We present a study of tip-enhanced Raman scattering on Au aerosol nanoparticles deposited on gold films. Under the tunneling current state, the Au tip and the Au aerosol nanoparticle form a narrow cavity, where large electromagnetic field enhancements are created to enhance Raman scattering enormously. Colorless *p*-thiocresol molecules are used as probe molecules. The estimated Raman enhancement is about nine orders of magnitude for the tip/particle configuration. © 2008 American Institute of Physics. [DOI: 10.1063/1.2837543]

Tip-enhanced Raman spectroscopy (TERS) is an emerging technology that combines Raman spectroscopy with scanning probe microscopy (SPM) to detect very small amounts of molecules or individual nanostructures on flat surfaces spectrally and spatially, which has recently attracted more and more scientific interests.^{1–8} Although Raman scattering is a very useful tool to obtain vibrational and structural information of molecules and condensed matters, the ordinary Raman scattering for small amounts of molecules is usually too weak to be detected. However, a dramatic Raman enhancement in TERS can occur if analyte molecules are located in a close vicinity of the curved surface of a sharp metal tip with a dimension in the nanometer scale.^{9,10} Except for the large Raman enhancement, TERS can also supply a high spatial resolution simultaneously with a sharp scanning metal tip.¹¹ Hence, TERS is becoming a powerful means to characterize molecules in the nanometer scale. Moreover, in contrast to surface-enhanced Raman spectroscopy (SERS), which was discovered three decades ago,¹² TERS can provide more controllable experimental environments to study Raman scattering of molecules with the assistance of the SPM technology,^{1,13} although TERS shares a similar mechanism for the Raman enhancement as SERS.^{14–16} Thus, TERS can have more advantages than SERS. However, the normal TERS is hardly to achieve the Raman enhancement as high as SERS when the SERS substrates are the aggregates of metal nanoparticles.^{17–19} The Raman enhancement by a metal tip only is rather limited, which is similar to the case of single metal nanoparticles. If flat metallic substrates are used, as illustrated in Fig. 1(a),^{20,21} the cavity between a metal tip and a metal surface can result in much stronger Raman enhancement than a single metal tip only.

In this paper, we explore the double-tip TERS technology to detect small nonresonant *p*-thiocresol molecules. As illustrated in Fig. 1(b), one tip is a normal scanning tunneling microscopy (STM) gold tip and the other is the fixed nanoprotusion on a flat gold surface, i.e., a gold nanoparticle made by aerosol technique in this study. Comparing the case of a gold tip on a flat gold surface, we find that more Raman

enhancement can be obtained in this new, double-tip configuration for TERS.

As illustrated in Fig. 1(b), a homemade STM is used to control the tip scanning over the sample and to obtain STM images. The scanning range of the STM is $2 \times 2 \mu\text{m}^2$. A Renishaw RA100 fiber-coupled Raman spectrometer is used to collect Raman signals from the scanning area. The coupling between the STM and the Raman spectrometer is through a Raman probe equipped with an Olympus $50\times$ objective lens, which is used for both focusing the laser on the tip and collecting the scattered light. The Raman probe can be manually adjusted in three dimensions with submicrometer accuracy, in order to obtain an efficient coupling to the STM. The key step is to judge if the laser is really focused on the apex of the STM tip and if the Raman light is collected efficiently. As shown in Fig. 2(a), when the tip and the mirror image of the tip in the substrate are clearly observed pointing to each other, the focus point of the objective can be easily adjusted exactly on the apex of the STM tip. In this case, the best coupling between the STM and the Raman spectroscope can be obtained. The wavelength of the excitation He–Ne laser is 632.8 nm and the laser power on the sample is about 2 mW in a focused area with a diameter of about $10 \mu\text{m}$.

The STM tips were obtained by etching the gold wires in a mixture of hydrochloric acid and ethanol, with a volume ratio of 1:1 similar to former studies.^{22,23} The etching conditions are crucial to obtain the desired shapes of the tips, which are important for the enhancement of the Raman intensity in TERS. In order to improve the reported

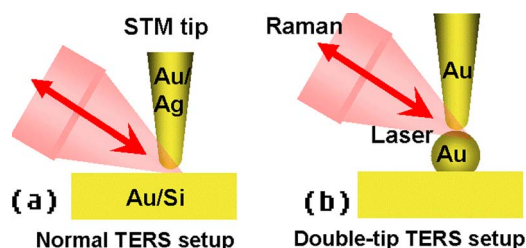


FIG. 1. (Color online) (a) Illustration of a conventional TERS setup. (b) Double-tip TERS setup used in this study.

^{a)}Electronic mail: hxxu@aphy.iphy.ac.cn.

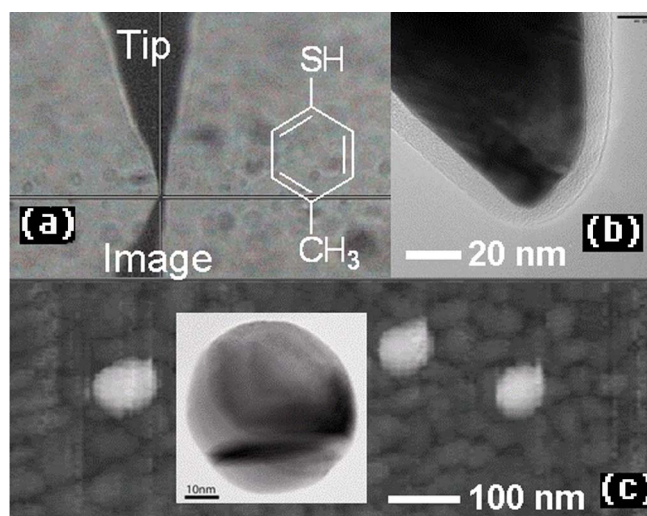


FIG. 2. (Color online) (a) Optical image of the STM tip on the silicon slide coated with a flat gold film and deposited with gold aerosol nanoparticles. (b) TEM image of a typical scanning tip used in the experiment. (c) STM image of gold aerosol nanoparticles deposited on a gold film. A TEM image of a typical gold nanoparticle is shown in the inset. The incident laser is tilted 30° to the surface. The inset in A shows the chemical structure of the *p*-thiocresol molecule.

methods,^{22,23} a low voltage of 1.3 V dc was applied to the gold wire as an anode electrode and a gold circle ring with a 5 cm diameter as a cathode electrode for the etching at the beginning. The etching current was ~ 3.5 mA, and the gold wire was immersed ~ 2 mm deep into the etching solution. This low voltage was chosen after investigating many experimental conditions. When the gold wire became 1/4 of the original size, after 12 min of etching, an ac voltage of 4 V was then applied to cut the thinner part of the gold wire to obtain a STM tip. The ac etching was found to be able to sharpen and smoothen the tip to improve its quality. A transmission electron microscopy (TEM) image of a typical gold tip is shown in Fig. 2(b), with a radius of the apex of about 10 nm.

The gold protrusions on the gold substrate were made by depositing aerosol gold nanoparticles on a flat gold film.²⁴ The sizes of the gold aerosol nanoparticles can be accurately selected by using a differential mobility analyzer.²⁴ Here, 50 nm diameter gold nanoparticles were used. A STM image of such gold nanoparticles on the gold film is shown in Fig. 2(c). The inset shows a TEM image of a typical gold nanoparticle. The substrate was then cleaned by hydrogen peroxide and sulfuric acid in a volume ratio of 1:3. The solution for cleaning was kept at 90°C by heating for 10 min in order to remove organic compounds on the substrate. This cleaning procedure will also etch the gold surface slightly. The substrate was then immersed into a $10^{-1}M$ *p*-thiocresol ethanol solution for 2 h and then rinsed with ethanol to get rid of nonadsorbed *p*-thiocresol molecules. *p*-thiocresol molecules (research grade) were obtained from Alfa Aesar. The chemical structure of the molecule is shown in the inset of Fig. 2(a). The thiol group in the molecule can be strongly adsorbed on the gold surface through the chemical bond between the sulfur atom and the gold atom.

Figure 3(a) shows a typical series of TERS spectra of adsorbed *p*-thiocresol molecules on the substrate collected from different points on a line scan by the STM. The scanning time step was set to 8 s, the same as the sum of the

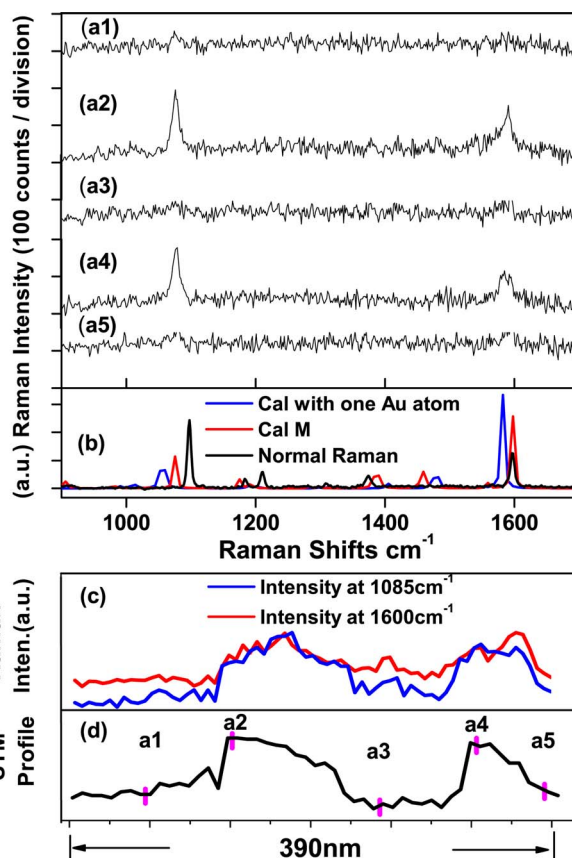


FIG. 3. (Color online) (a) Series of Raman spectra of *p*-thiocresol molecules collected from the positions marked in the STM profile in (d). (b) Raman spectrum of bulk *p*-thiocresol molecules (blue) and calculated spectra of *p*-thiocresol molecule with (green) and without (red) one Au atom substituting the H atom in the thiol group. (c) Scanned Raman intensity profiles at peak positions of 1085 cm^{-1} (green) and 1600 cm^{-1} (red), respectively, correspond to the same scanning of the STM profile in (d). (d) STM profile where the Raman spectra are scanned.

accumulation time and the recording time of the Raman spectrometer. Hence, both the spectral scanning and the spatial scanning were synchronized. Significant TERS spectra of *p*-thiocresol molecules with two strong characteristic vibrational peaks at 1085 and 1600 cm^{-1} can be acquired at points A2 and A4, but almost no Raman signals at points A1, A3, and A5. The bulk Raman spectrum taken from a crystal-like powder, shown in Fig. 3(b), verifies that the TERS spectra are truly from *p*-thiocresol molecules. The slight difference between TERS and bulk spectra may be caused by the fact that the state of chemisorbed *p*-thiocresol molecules may differ from the bulk molecules in the crystal. The calculated Raman spectrum and calculated TERS spectrum of single *p*-thiocresol molecule also give similar evidence for TERS spectra of *p*-thiocresol molecules. For quantum chemical calculations, the geometry optimizations and frequency analyses of all models for the ground states were performed with density functional theory by GAUSSIAN 03 suite,²⁵ where B3LYP functional is used with different basis sets of 6-31G(D) and LanL2DZ for a *p*-thiocresol molecule only and a pair of *p*-thiocresol molecule and Au atom, respectively.

Comparing the low peak intensity of 1600 cm^{-1} at point A3 with the peak height of ~ 20 counts to the peak intensity at point A2 with the peak height of ~ 100 counts, the Raman enhancement at A2 is about five times larger than that at A3.

At the low frequency peak of 1085 cm^{-1} , the enhancement at A2 is estimated to be about one order larger than that at A3, which Raman peak intensity is very low. The different enhancement factors could be caused by the different couplings between the field and metal-molecule polarizability depending on symmetry for different vibrational bands. The spectrum at point A4 is similar to that at A2, while the very weak Raman spectra at points A1 and A5 are similar to the case of A3.

As seen in the STM topological profile in Fig. 3(d), it is interesting that points A2 and A4 are both located at the top positions of the profile, which correspond to the apexes of two gold nanoparticles, respectively, while points A1, A3, and A5 are located on the flat gold film only. We plot the peak intensities of the two Raman peaks at 1085 and 1600 cm^{-1} for all different scanning points, respectively, as shown in Fig. 3(c). The profiles of the Raman peak intensities are very similar to the corresponding STM topological profile.

This clearly shows that the Raman intensity can increase dramatically when the STM gold tip moves close to and onto the gold nanoparticles. It has been demonstrated that the strong electromagnetic coupling between two close-packed metal nanoparticles can generate enormous field enhancement that favors SERS up to the single molecule level.^{17–19} In a similar fashion, the electromagnetic coupling between the sharp STM gold tip and the gold protrusion on the substrate may cause enormous field enhancement in the cavity between two “tips,” which favors TERS as well.

The estimated absolute enhancement of TERS can be obtained by comparing the TERS intensity of *p*-thiocresol molecules with the normal Raman intensity of the same molecules. The density of *p*-thiocresol adsorbed on the substrate in our experimental conditions (under 2 h incubation) can be estimated to be submonolayer. By assuming a similar absorption behavior as 9-mercaptoanthracene molecules,²⁶ but with two times smaller in size, we estimated the coverage of *p*-thiocresol molecule for a dense monolayer to be about 4 molecules/nm². The TERS intensities are mainly contributed by the molecules within the area beneath the apex of the tip, which is estimated to be about 100 nm². The other area under the laser illumination can be ignored, where the enhancement is much lower than the area underneath the apex of the tip. Since there are no Raman signals if the tip is retracted, this observation justifies the above estimation. While the same laser spot illuminates the crystal of *p*-thiocresol molecules, the normal Raman intensity is contributed by a certain amount of molecules. Since the volume of one *p*-thiocresol molecule in the crystal is about 300 Å³, the diameter of the illuminated area is about 10 μm, and the laser penetration depth is about 5 μm, the number of the *p*-thiocresol molecules contributing to the bulk Raman spectrum is estimated as $\sim 1.3 \times 10^{12}$. For the Raman peak intensity at 1085 cm^{-1} , the one for TERS is about 200 counts, which is contributed by 400 molecules, while the one for the normal Raman under the same experimental condition is about 1350 counts, which is contributed by 1.3×10^{12} molecules. The TERS enhancement is estimated as $(200/400)/(1350/1.3 \times 10^{12}) \approx 6 \times 10^8$ for a dense *p*-thiocresol molecule layer. Considering the short incubation time in our experiment, only 1/4 of the duration required for a dense layer, the coverage of the molecules should be much

less than a dense layer. Hence, the TERS enhancement can be estimated to be more than the order of 10^9 .

In summary, we report a method for achieving larger Raman enhancement by double-tip TERS: one tip is a scanning gold tip and the other one is the gold nanoparticle adsorbed on a flat gold surface as a fixed tip. In most other TERS experiments, dye molecules were often used as probe molecules, which have a larger Raman cross section than small nonresonant molecules. Hence, they are easier to “see” on the flat gold substrate with normal TERS setup, but this is not the case for small nonresonant molecules. In our work, we have demonstrated that with the double-tip configuration of TERS, Raman spectra of *p*-thiocresol molecules, colorless small molecules, can easily be observed.

We thank Mariusz Graczyk at Lund University for sample preparations, Xuedong Bai at Institute of Physics of CAS and Lisa Karlsson at Lund University for TEM imaging, and Songbo Wan at Institute of Physics of CAS for calculating Raman spectra. This work is supported by NSFC under Grant No. 10625418, MOST under Grant No. DFB02020, the project of “Bairenjihua” of CAS, and the Swedish Research Council (VR).

¹B. Pettinger, *Top. Appl. Phys.* **103**, 217 (2006); P. Verma, Y. Inouye, and S. Kawata, *Top. Appl. Phys.* **103**, 241 (2006).

²R. Stöckle, Y. Suh, V. Deckert, and R. Zenobi, *Chem. Phys. Lett.* **318**, 131 (2000).

³M. S. Anderson, *Appl. Phys. Lett.* **76**, 3130 (2000).

⁴N. Hayazawa, Y. Inouye, Z. Sekkat, and S. Kawata, *Chem. Phys. Lett.* **335**, 369 (2001).

⁵N. Hayazawa, T. Yano, H. Watanabe, Y. Inouye, and S. Kawata, *Chem. Phys. Lett.* **376**, 174 (2003).

⁶B. Pettinger, G. Picardi, R. Schuster, and G. Ertl, *Single Mol.* **3**, 285 (2002).

⁷H. Watanabe, Y. Ishida, N. Hayazawa, Y. Inouye, and S. Kawata, *Phys. Rev. B* **69**, 155418 (2004).

⁸B. Pettinger, B. Ren, G. Picardi, R. Schuster, and G. Ertl, *Phys. Rev. Lett.* **92**, 096101 (2004).

⁹J. T. Krug, E. J. Sanchez, and X. S. Xie, *J. Chem. Phys.* **116**, 10895 (2002).

¹⁰M. Micic, N. Klymyshyn, Y. D. Suh, and H. P. Lu, *J. Phys. Chem. B* **107**, 1574 (2003).

¹¹A. Hartschuh, E. J. Sánchez, X. S. Xie, and L. Novotny, *Phys. Rev. Lett.* **90**, 095503 (2003).

¹²D. Jeanmaire and R. Van Duyne, *J. Electroanal. Chem. Interfacial Electrochem.* **84**, 1 (1977).

¹³H. Watanabe, N. Hayazawa, Y. Inouye, and S. Kawata, *J. Phys. Chem. B* **109**, 5012 (2005).

¹⁴M. Moskovits, *Rev. Mod. Phys.* **57**, 783 (1985).

¹⁵K. Kneipp, H. Kneipp, I. Itzkan, R. Dasari, and M. Feld, *Chem. Rev. (Washington, D.C.)* **99**, 2957 (1999).

¹⁶G. C. Schatz and R. V. Duyne, in *Handbook of Vibrational Spectroscopy*, edited by J. M. Chalmers and P. R. Griffiths (Wiley, New York, 2002).

¹⁷H. X. Xu, E. Bjerneld, M. Käll, and L. Börjesson, *Phys. Rev. Lett.* **83**, 4357 (1999).

¹⁸A. M. Michaels, J. Jiang, and E. Brus, *J. Phys. Chem. B* **104**, 11965 (2000).

¹⁹H. X. Xu, J. Aizpurua, M. Käll, and P. Apell, *Phys. Rev. E* **62**, 4318 (2000).

²⁰K. F. Domke, D. Zhang, and B. Pettinger, *J. Am. Chem. Soc.* **128**, 14721 (2006).

²¹W. H. Zhang, B. S. Yeo, T. Schmid, and R. Zenobi, *J. Phys. Chem. C* **111**, 1733 (2007).

²²B. Ren, G. Picardi, and B. Pettinger, *Rev. Sci. Instrum.* **75**, 837 (2004).

²³D. Roy, J. Wang, and M. Welland, *Faraday Discuss.* **132**, 215 (2006).

²⁴M. H. Magnusson, K. Deppert, J.-O. Malm, J.-O. Bovin, and L. Samuelsson, *Nanostruct. Mater.* **12**, 45 (1999).

²⁵GAUSSIAN 03, Revision B.05, Gaussian, Inc., Pittsburgh PA, 2003.

²⁶R. Dou, Q. Xue, W. Yang, and A. Jen, *Langmuir* **22**, 3049 (2006).